Quaternary Research **55**, 235–245 (2001)
doi:10.1006/qres.2000.2211, available online at http://www.idealibrary.com on IDEAL®

Rates of Sediment Supply to Arroyos from Upland Erosion Determined Using *in Situ* Produced Cosmogenic ^{10}Be and ^{26}Al

Erik M. Clapp,[1] Paul R. Bierman, and Kyle K. Nichols

University of Vermont, School of Natural Resources and Department of Geology, Burlington, Vermont 05401

Milan Pavich

United States Geological Survey, Reston, Virginia 22092

and

Marc Caffee

Center for Accelerator Mass Spectrometry, Lawrence Livermore National Laboratory, Livermore, California 94550

Received June 29, 1999

Using ^{10}Be and ^{26}Al measured in sediment and bedrock, we quantify rates of upland erosion and sediment supply to a small basin in northwestern New Mexico. This and many other similar basins in the southwestern United States have been affected by cycles of arroyo incision and backfilling several times in the past few millennia. The sediment generation (275 ± 65 g m^{-2} yr^{-1}) and bedrock equivalent lowering rates (102 ± 24 m myr^{-1}) we determine are sufficient to support at least three arroyo cycles in the past 3,000 years, consistent with rates calculated from a physical sediment budget within the basin and regional rates determined using other techniques. Nuclide concentrations measured in different sediment sources and reservoirs suggest that the arroyo is a good spatial and temporal integrator of sediment and associated nuclide concentrations from throughout the basin, that the basin is in steady-state, and that nuclide concentration is independent of sediment grain size. Differences between nuclide concentrations measured in sediment sources and reservoirs reflect sediment residence times and indicate that subcolluvial bedrock weathering on hillslopes supplies more sediment to the basin than erosion of exposed bedrock.

INTRODUCTION

Determining rates of sediment generation is important for understanding landscape evolution and landscape response to changes in climate and land use. On the semiarid, southern Colorado Plateau, changes in climate and land use have significantly influenced landscape evolution (Leopold *et al.*, 1966; Bull, 1991; Gellis *et al.*, 2000). For example, during the Holocene, the Rio Puerco underwent multiple cycles of aggradation and gullying (Bryan, 1925; Love, 1986; Love and Young, 1983). The arroyo network of this 1600 km^2 basin last began incising during the late 1800s (Bryan, 1925; Aby, 1997; Gellis and Elliott, 1998); however, since ~1940, these arroyos, with the exception of some low-order channels that continue to migrate headward (Fig. 1), have been aggrading (Gellis *et al.*, 2000; Gellis and Elliott, 1998; Elliott *et al.*, 1999).

Arroyo incision and subsequent backfilling form a cycle that has repeated itself several times in the past three millennia (Love and Young, 1983; Love, 1986; Gellis *et al.*, 2000). Cycles of arroyo cutting and filling require a sediment source sufficient to refill the arroyo following periods of incision (Cooke and Revees, 1976). There are two primary sources for this sediment, erosion of the uplands and aeolian input. Recent sediment-trap data (Gellis *et al.*, 2000) indicate that aeolian transport is responsible for less than 1% of the total sediment moving in our study area. Therefore, in this paper we focus on rates of sediment generation from bedrock erosion in the uplands.

In order to quantify long-term sediment generation rates within Arroyo Chavez (Fig. 1 and 2), a tributary of the Rio Puerco, we measured *in situ* produced cosmogenic ^{10}Be and ^{26}Al in the quartz fraction of 16 sediment and 3 bedrock samples. We use the drainage network of the basin as an integrator of sediment from throughout the basin and interpret ^{10}Be and ^{26}Al concentrations in stream channel sediments as representative of basinwide average concentrations (Bierman and Steig, 1996). Our methods are better suited to determining long-term sediment generation rates than traditional sediment monitoring because the accumulation of nuclides integrates rates over thousands of years, a time span over which short-term (decadal) fluctuations in climate and sediment generation will not be significant. Our results demonstrate the value of cosmogenic isotopes in

[1] Current address: C/O SME, 4 Blanchard Road, Box 85A, Cumberland Center, Maine 04021. E-mail: emc@smemaine.com. Fax: (207) 829-5692.

0033-5894/01 $35.00

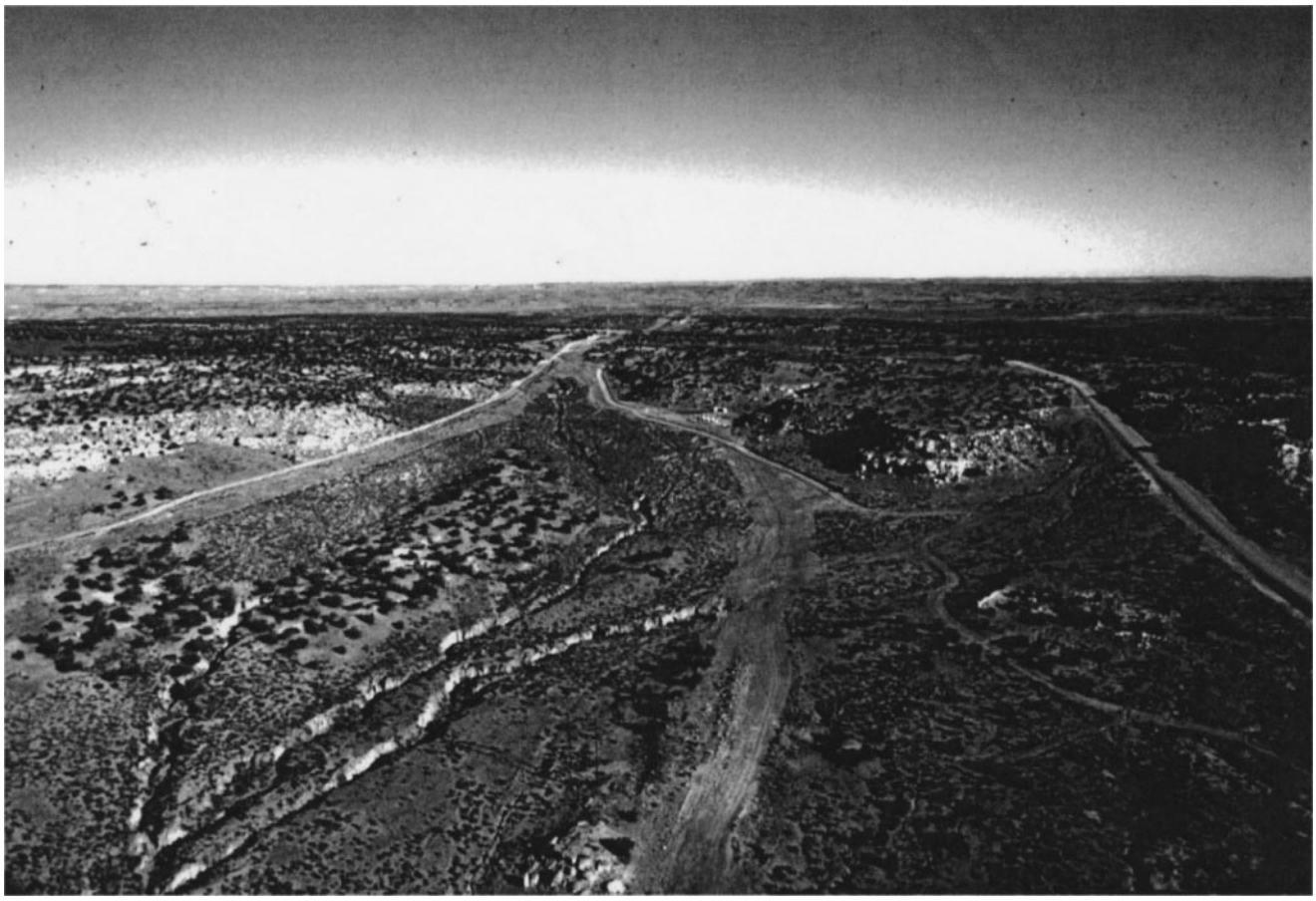

FIG. 1. Arroyo Chavez subbasin, southeastern edge of the Colorado Plateau. Looking north into the subbasin. Northern boundary of the watershed is far center of the photograph where roads join. Front of photograph is 2.5 km across.

providing rapid estimates of long-term sediment generation rates and illustrate one of the many different spatial scales at which the method may be applied.

GEOMORPHIC SETTING

Arroyo Chavez occupies a small basin (17.3 km^2) on the Colorado Plateau ~2 km above sea level (Fig. 2). The climate is semiarid (mean annual precipitation, 377 mm; Gellis *et al.*, 2000). Our study focuses on the headwaters, a 1.1 km^2 subbasin underlain primarily by homogeneous, arkosic sandstone. The basin is characterized by more resistant, flat-lying sandstones that form mesa tops, overlying less resistant, hillslope-forming sandstones and shales (Fig. 3).

Regolith is present on most hillslope and mesa surfaces. The mesa tops have a thin, 0- to 20-cm veneer of fine-grained, quartz-rich sand and silt (69% $< 2000\ \mu$m). The hillslopes have similar colluvial deposits generally less than 30 cm deep ($\mu = 15.3 \pm 14.3$ cm, $n = 50$); bedrock hollows contain deposits as deep as 90 cm. At the base of some hillslopes, gently sloping alluvial fans have formed (<5 m thick). The fan deposits are weakly stratified, are the same color and texture as the hillslope colluvium, and do not contain distinct paleosols, thus suggesting rapid or steady aggradation.

Material shed from the basin hillslopes is deposited on alluvial fans and on the valley bottom. The valley fill is <5 m thick based on bedrock outcrops observed at the bottom of the arroyo. The channel is 1 to >4 m wide. The basin alluvium comprises alternating layers of fine sand, medium to coarse sand, and coarse sand with occasional pebbles. It is weakly cemented by calcium carbonate, crudely stratified, and there are no distinct soil horizons.

IN SITU PRODUCED COSMOGENIC ISOTOPES IN SEDIMENTS

^{10}Be and ^{26}Al are produced in quartz from the interaction of secondary cosmic rays (primarily high-energy neutrons) with Si and O (Lal, 1988). These cosmogenic radionuclides accumulate most rapidly in sediment and bedrock residing at or near Earth's surface (<3 m depth); accumulation or "production" rates decrease exponentially with depth (Lal, 1988). An inverse relationship exists between the rate at which sediment

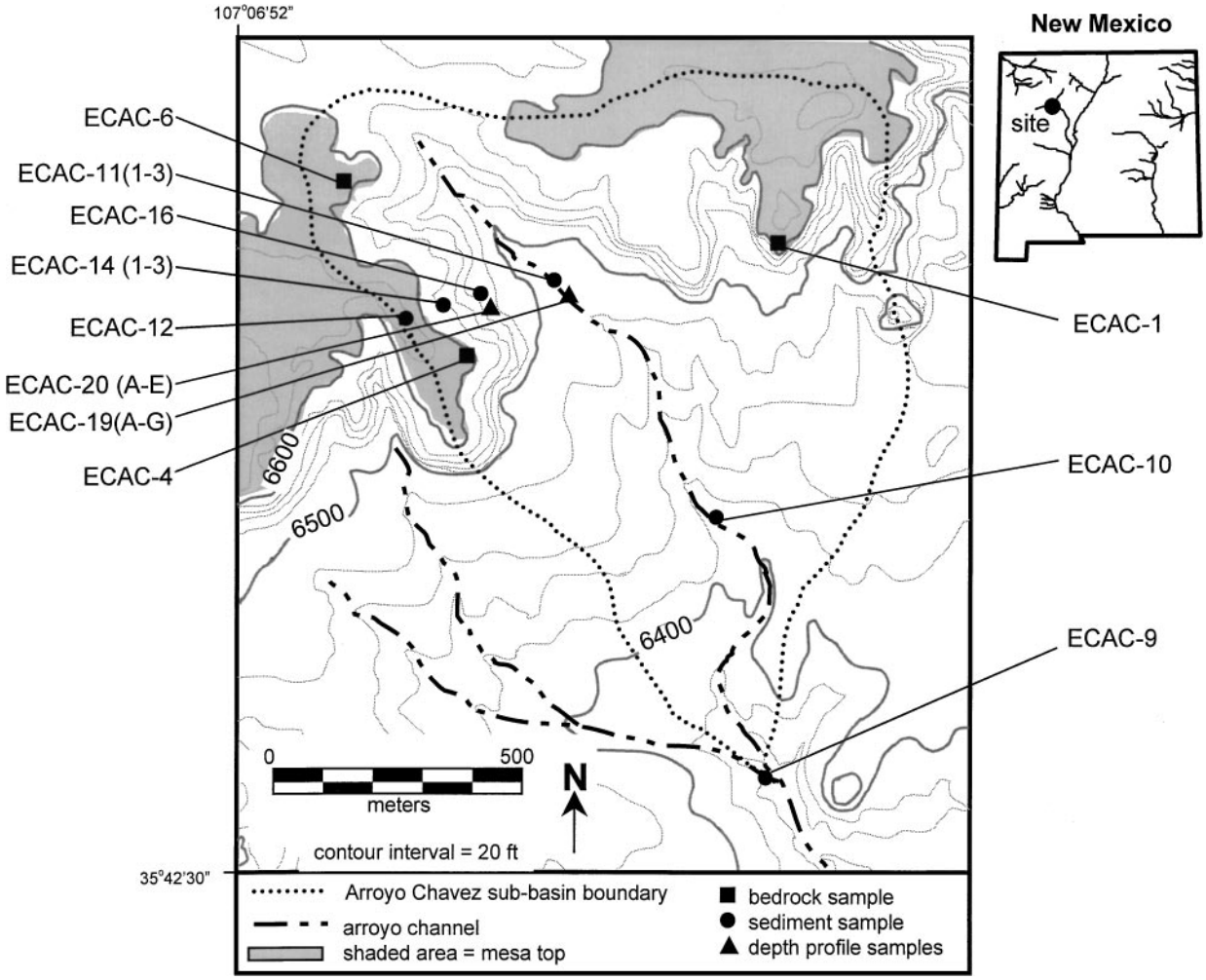

FIG. 2. Topography of the Arroyo Chavez subbasin. Samples are designated with squares (bedrock), circles (channel sediment and colluvium), and triangles (depth profiles). Shaded areas represent mesa tops. Sample ECAC 8-2 is located in the main channel, approximately 1200 m south of the southern edge of the map. Map adapted from 7.5-min San Luis Quadrangle Map (U.S. Geological Survey, 1961).

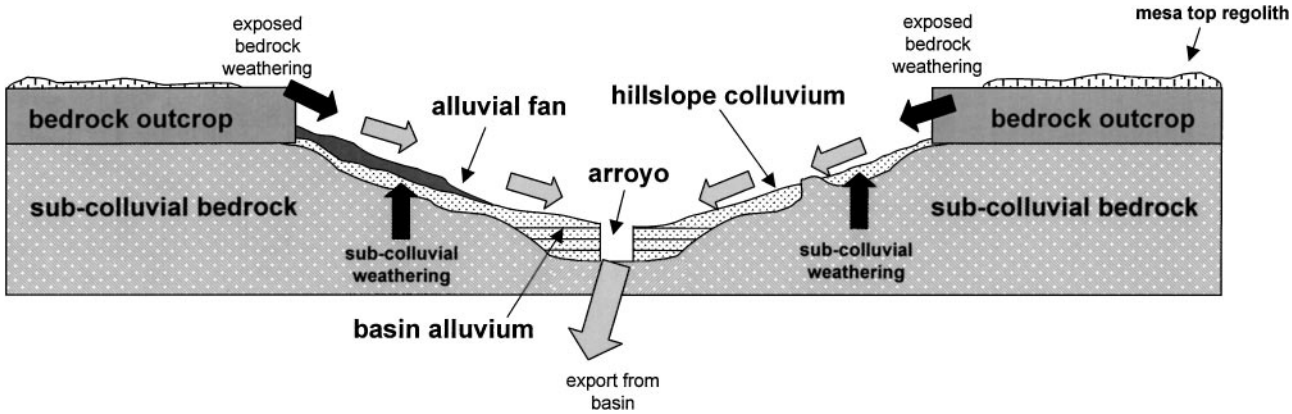

FIG. 3. Schematic cross section of the Arroyo Chavez subbasin depicting the general flow of sediment from sources (weathering of exposed bedrock outcrops and subcolluvial bedrock) to the reservoirs (hillslope colluvium, alluvial fan, and basin alluvium) and the transport of sediment out of the basin. Black arrows represent bedrock weathering. Gray arrows represent sediment transport.

is being generated and transported from a drainage basin (erosion) and the concentration of *in situ* produced cosmogenic nuclides in that sediment (Lal, 1991; Brown *et al.*, 1995a; Bierman and Steig, 1996; Granger *et al.*, 1996). The relationship between nuclide concentration and sediment generation rate has been quantified using interpretive models (Lal, 1991; Bierman and Steig, 1996); nuclide measurements have been used to estimate time-integrated rates of sediment generation, bedrock lowering, and sediment yield (e.g., Bierman and Turner, 1995; Brown *et al.*, 1995a; Granger *et al.*, 1996; Small *et al.*, 1999).

The Arroyo Chavez basin can be thought of as a series of reservoirs (hillslope colluvium, alluvial fan sediment, basin alluvium, and channel sediment) through which sediment flows en route from bedrock source areas to the basin outlet (Fig. 3). During transport and storage, nuclides accumulate and record the relative time of sediment residence. We measured ^{10}Be and ^{26}Al concentrations in individual reservoirs to test assumptions used to interpret cosmogenic nuclide concentrations in sediment. Differences between nuclide concentrations in different reservoirs can be used to track sediment contributions.

The interpretive model used to determine sediment generation rates from cosmogenic nuclides measured in sediments (Brown *et al.*, 1995a; Bierman and Steig, 1996; Granger *et al.*, 1996) is based on a balance between nuclides produced in or entering a drainage basin and those leaving the basin (Fig. 4). To calculate meaningful sediment generation rates from nuclide abundances, two assumptions must be valid: the total reservoir of cosmogenic nuclides (C) within the basin must remain constant over time (steady state) and the sediment leaving the basin must be well mixed.

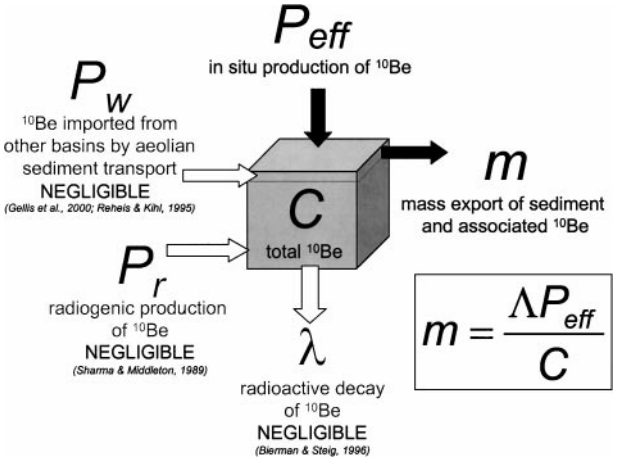

FIG. 4. Balance of cosmogenic ^{10}Be in the Arroyo Chavez basin (adapted from Bierman and Steig, 1996). Unshaded arrows represent nuclide inputs or outputs which are negligible. Black arrows represent nuclide inputs or outputs which control the total nuclide inventory (C) of the basin. Basinwide nuclide inventory is controlled by *in situ* production (P_{eff}) and the rate that nuclides are carried away with sediment through mass export (m). The characteristic attenuation length for fast neutrons (Λ) is constant (165 g cm^{-2}).

METHODS

Sample Collection

Sediment and bedrock samples were collected from the reservoirs described in the previous sections (Table 1, Figs. 2 and 3). We collected three bedrock samples from ridges surrounding the subbasin. Three evenly spaced sediment samples were collected along a hillslope transect 320 m long; each was an integration of the 10- to 20-cm depth of hillslope colluvium. We assumed complete mixing of sediment would occur for such shallow cover. Four homogenized sediment samples were collected from different sites along the bottom of the active stream channel (Fig. 2). Additionally, four alluvial fan sediment samples were collected from a 4-m-deep vertical profile (Fig. 2). Fan samples were collected at approximately 100-cm depth increments; each sample was integrated over a 10-cm depth range. A similar 3.8-m-deep profile was sampled where the basin alluvium was exposed by the main stem of Arroyo Chavez (Fig. 2).

Sample Preparation

All sediment samples were prewashed in HCl to remove carbonate. Five samples (ECAC-11, -14, -19A, -19D and -J19G) were sieved to test the relationship between grain size and nuclide concentration. The remaining 12 sediment samples were sieved to yield only the 250- to 1000-μm size fraction. All particles smaller than 125 μm were discarded to minimize aeolian contribution (Reheis and Kihl, 1995). Samples were heated and ultrasonically etched to isolate 20 to 30 g of pure quartz (Kohl and Nishiizumi, 1992), which was dissolved in HF containing 250 μg of Be carrier. Be and Al were then isolated using ion chromatography, and isotopic ratios were determined by accelerator mass spectrometry at Lawrence Livermore National Laboratory. Al was measured in duplicate aliquots by inductively coupled argon plasma spectrometry—optical emission.

Data Interpretation

The ^{10}Be and ^{26}Al measured in 26 samples from 12 locations (Tables 1 and 2, Fig. 5) are well correlated. The time scale over which our samples could have been buried is too short to affect the ^{26}Al/^{10}Be ratio, thus the ^{26}Al measurements can be considered replicates of the ^{10}Be measurements. Both the ^{10}Be and ^{26}Al measurements are used in the calculation of average erosion and sediment generation rates. To streamline data presentation, our discussion focuses on the ^{10}Be data.

Production rates of 6.03 and 36.8 (atoms g^{-1} yr^{-1}) for ^{10}Be and ^{26}Al, respectively (Nishiizumi *et al.*, 1989), were used in the calculation of erosion rates. The production rates were scaled for latitude and elevation according to Lal (1991), assuming no muon production (Brown *et al.*, 1995b) and 20% uncertainty (Clark *et al.*, 1995). No corrections have been made for quartz enrichment (Small *et al.*, 1999) as our quartz-yield data indicate ~25% quartz content for bedrock samples and ~22% for sediment samples. All statistical comparisons were made using

TABLE 1
Locations and Descriptions of Samples from Arroyo Chavez Basin, New Mexico

Sample	Latitude[a]	Longitude[a]	Elevation[b] (km)	Sample type	Grain size (μm)
ECAC 1	N35°42.301′	W107°06.063′	2.030	bedrock	not applicable
ECAC 4	N35°42.106′	W107°06.487′	2.042	bedrock	not applicable
ECAC 6	N35°42.359′	W107°06.619′	2.042	bedrock	not applicable
ECAC 8-2	N35°40.163′	W107°05.415′	1.951	channel sediment	500–1000
ECAC 9	N35°41.565′	W107°06.018′	1.963	channel sediment	250–1000
ECAC 10	N35°41.941′	W107°06.068′	1.972	channel sediment	250–1000
ECAC 11-1	N35°42.246′	W107°06.415′	1.978	channel sediment	125–500
ECAC 11-2	N35°42.246′	W107°06.415′	1.978	channel sediment	500–1000
ECAC 11-3	N35°42.246′	W107°06.415′	1.978	channel sediment	1000
ECAC 12	N35°42.179′	W107°06.652′	2.006	hillslope colluvium	250–1000
ECAC 14-1	N35°42.188′	W107°06.610′	2.003	hillslope colluvium	125–500
ECAC 14-2	N35°42.188′	W107°06.610′	2.003	hillslope colluvium	500–1000
ECAC 14-3	N35°42.188′	W107°06.610′	2.003	hillslope colluvium	>1000
ECAC 16	N35°42.211′	W107°06.557′	1.998	hillslope colluvium	250–1000
ECAC 19A-1	N35°42.271′	W107°06.423′	1.984	basin alluvium	125–500
ECAC 19A-2	N35°42.271′	W107°06.423′	1.984	basin alluvium	500–1000
ECAC 19C	N35°42.271′	W107°06.423′	1.985	basin alluvium	250–1000
ECAC 19D-1	N35°42.271′	W107°06.423′	1.986	basin alluvium	125–500
ECAC 19D-2	N35°42.271′	W107°06.423′	1.986	basin alluvium	500–1000
ECAC 19E	N35°42.271′	W107°06.423′	1.986	basin alluvium	250–1000
ECAC 19G	N35°42.271′	W107°06.423′	1.987	basin alluvium	250–1000
ECAC 19G-3	N35°42.271′	W107°06.423′	1.987	basin alluvium	>1000
ECAC 20A	N35°42.271′	W107°06.423′	1.991	alluvial fan sediment	250–1000
ECAC 20B	N35°42.271′	W107°06.423′	1.992	alluvial fan sediment	250–1000
ECAC 20C	N35°42.271′	W107°06.423′	1.992	alluvial fan sediment	250–1000
ECAC 20E	N35°42.271′	W107°06.423′	1.995	alluvial fan sediment	250–1000

[a] Measured using Garmin 75 hand-held GPS.
[b] Measured using hand-held altimeter calibrated to local benchmark.

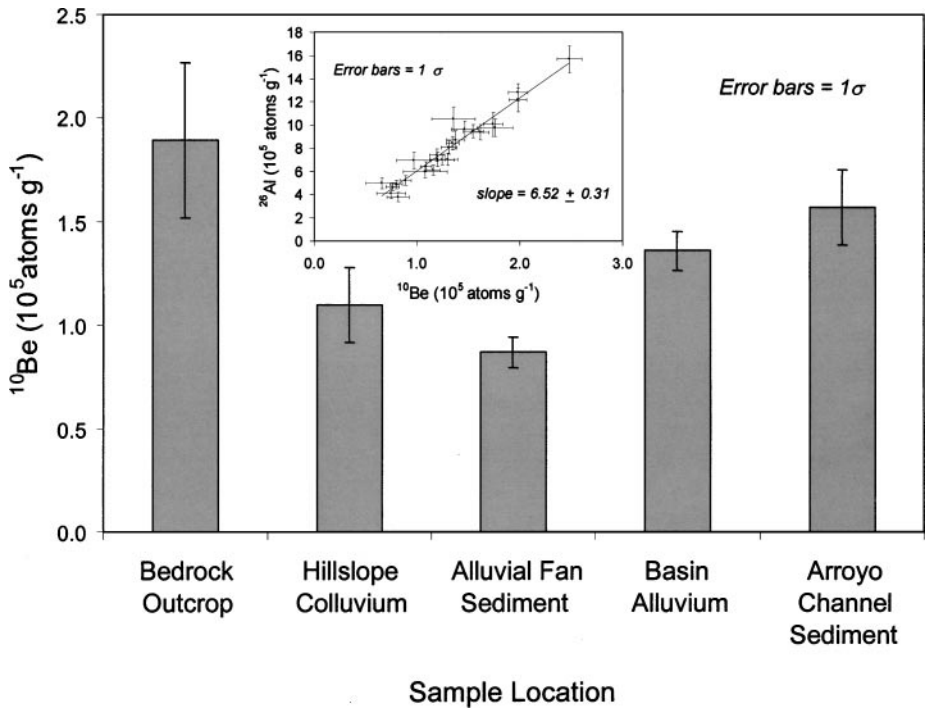

FIG. 5. Average ^{10}Be concentrations for individual sediment reservoirs in the Arroyo Chavez subbasin. Inset shows ^{10}Be vs ^{26}Al concentrations for all Arroyo Chavez samples. Best-fit line has a slope of 6.52 ± 0.31 (based on methods of York (1969)), consistent with the currently accepted ^{26}Al : ^{10}Be production ratio of ~6 : 1 (Nishiizumi *et al.*, 1989).

TABLE 2
Concentrations of ^{10}Be and ^{26}Al Measured in Samples from Arroyo Chavez Basin, New Mexico

Sample	^{10}Be (10^5 atoms g^{-1})	^{26}Al (10^5 atoms g^{-1})
	Bedrock outcrops	
ECAC1	1.19 ± 0.07	7.43 ± 0.53
ECAC4	2.48 ± 0.12	15.70 ± 1.15
ECAC6	1.98 ± 0.09	12.82 ± 0.75
Average	*1.89 ± 0.37*	*11.98 ± 2.42*
Bedrock nuclide abundance > hillslope ($P = 0.08$) and fan ($P = 0.06$)[c]		
	Hillslope Colluvium	
ECAC12	1.31 ± 0.08	8.07 ± 0.57
ECAC14-1	0.66 ± 0.15	4.99 ± 0.47
ECAC14-2	0.82 ± 0.11	3.80 ± 0.39
ECAC14-3	0.75 ± 0.14	4.11 ± 0.44
ECAC16	1.24 ± 0.12	7.02 ± 0.47
Average[a]	*1.10 ± 0.18*	*6.46 ± 1.12*
Hillslope nuclide abundance < bedrock ($P = 0.08$) and channel ($P = 0.06$)[c]		
	Alluvial fan profile	
ECAC20A	0.76 ± 0.06	4.69 ± 0.36
ECAC20B	1.09 ± 0.06	6.42 ± 0.43
ECAC20C	0.80 ± 0.06	4.90 ± 0.38
ECAC20E	0.89 ± 0.06	5.24 ± 0.40
Average[b]	*0.87 ± 0.07*	*5.23 ± 0.38*
Fan nuclide abundance < bedrock ($P = 0.06$), basin ($P = 0.001$), and channel ($P = 0.01$)[c]		
	Basin alluvium profile	
ECAC19A-1	1.76 ± 0.17	9.78 ± 0.75
ECAC19A-2	1.36 ± 0.21	10.53 ± 1.05
ECAC19C	1.55 ± 0.10	9.46 ± 0.60
ECAC19D-1	1.46 ± 0.13	9.65 ± 0.73
ECAC19D-2	1.62 ± 0.08	9.38 ± 0.66
ECAC19E	1.37 ± 0.09	8.73 ± 0.77
ECAC19G	1.16 ± 0.07	6.13 ± 0.45
ECAC19G-3	0.97 ± 0.17	6.99 ± 0.71
Average[a,b]	*1.36 ± 0.09*	*8.51 ± 0.62*
Basin nuclide abundance > fan ($P = 0.06$)[c]		
	Arroyo channel sediments	
ECAC8-2	1.74 ± 0.09	10.07 ± 1.05
ECAC9	1.35 ± 0.06	8.44 ± 0.58
ECAC10	1.98 ± 0.09	12.19 ±1.04
ECAC11-1	1.30 ± 0.10	7.05 ± 0.53
ECAC11-2	1.20 ± 0.08	7.06 ± 0.61
ECAC11-3	1.08 ± 0.21	5.98 ± 0.52
Average[a]	*1.57 ± 0.18*	*9.35 ± 1.17*
Channel nuclide abundance > hillslope ($P = 0.06$) and fan ($P = 0.01$)[c]		

Note. Samples ending with -1, -2, and -3 are grain-size fractions (125–500, 500–1000, and >1000 μm, respectively). Measurements are average $\pm 1\sigma$ analytical error (Lawerence Livermore National Laboratory). Averages reported with ±1 standard error of the mean.

[a] Size fractions were averaged together before total averages were calculated.

[b] Averages for profiles are weighted by sampled depth interval.

[c] Statistical comparisons between sediment reservoirs made using independent *t*-test assuming unequal variance at 90% confidence interval ($\alpha = 0.1$).

a confidence interval of 90% and independent *t*-tests assuming unequal variance (Ott, 1993).

RESULTS AND DISCUSSION

Isotopic data indicate that Arroyo Chavez sediment is well mixed and that the basin is in steady state. Based on this evidence, we use the data to determine basinwide sediment generation rates.

Model Evaluation

Fluvial Integration of Basin Sediments

Sediments generated from the upland hillslopes and bedrock outcrops are mixed together by bioturbation, rain splash, and freeze–thaw. In the Arroyo Chavez basin, there are few direct pathways for upland sediment to enter the main stem of the arroyo without first mixing with hillsope colluvium. Mixing and integration of sediment and associated nuclides continues as material is transported and deposited in alluvial fans and valley alluvium. As the channel meanders across the basin, the arroyo incises through the basin alluvium, and arroyo walls collapse into the channel. Subsurface piping removes sediment from the valley fill and delivers it to the arroyo channel (at the time of sampling, more than five recent wall failures and hundreds of subsurface pipes were observed along the channel above the sampling sites). These processes mix sediment from much of the width and depth of the basin as well as the length of the channel. Therefore, the channel-sediment nuclide concentration and the resultant erosion and sediment generation rates we calculate are integrated both spatially (as described above) and temporally by cutting through the depth profile that represents a long-term record of nuclide concentrations.

The ^{10}Be data we have collected are consistent with the above description. The average ^{10}Be concentration measured in the stream-channel sediment ($1.57 \pm 0.18 \times 10^5$ atoms g^{-1}) is statistically indistinguishable from the average concentration of the basin alluvium profile samples, weighted by percentage of profile depth ($1.36 \pm 0.09 \times 10^5$ atoms g^{-1}). Additionally, there are only slight differences ($<2\sigma$) between the nuclide concentration of the channel sediment and other sediment reservoirs throughout the basin (Table 2) with the exception of the alluvial fan, which occupies only a small portion (<3%) of the basin. Channel-sediment nuclide concentrations are thus representative of basinwide sediment nuclide concentrations.

Steady-State Erosion and Nuclide Inventory

Calculation of basinwide erosion rates from sediment nuclide concentrations in well-mixed alluvium requires that a basin have a steady-state nuclide inventory for which the flux of nuclides into the basin equals the flux out (Bierman and Steig, 1996). A basin with a steady-state nuclide inventory (constant C) must be losing sediment mass (m) and associated nuclides at a constant rate (steady-state erosion). Although we cannot directly

determine if a basin has a steady-state nuclide inventory, we can use steady-state erosion as a proxy. Several lines of evidence suggest that the Arroyo Chavez basin is eroding steadily: down-basin isotopic homogeneity, depth-profile isotopic homogeneity, and steady-state deposition of basin alluvium.

Down-basin isotopic homogeneity. Isotopic concentrations in sediment reservoirs throughout the Arroyo Chavez basin are similar (Table 2 and Fig. 5), suggesting steady-state erosion without long periods of storage. Particles systematically approach the landscape surface and accumulate nuclides at similar rates throughout the basin. Differences in isotopic concentrations between sample locations can be attributed to slight, local variations (at the 1000-m^2 scale) in erosion rates related to differences in lithology, catchment size, and slope. Slightly higher nuclide concentrations in basin alluvium ($1.36 \pm 0.09 \times 10^5$ atoms g^{-1}) and channel sediment ($1.57 \pm 0.18 \times 10^5$ atoms g^{-1}) compared to hillslope colluvium ($1.10 \pm 0.18 \times 10^5$ atoms g^{-1}) are likely the effect of nuclide accumulation integrated over several thousand years following deposition.

By contrast, a basin that was undisturbed by erosion for thousands of years (i.e., a long period of nuclide accumulation), and was only recently stripped of its upland sediment cover, should have deposits of high-concentration sediment in alluvial-fan and basin alluvium, leaving newly exposed (previously shielded from cosmic rays), low-concentration bedrock and sediment in the uplands. However, exposed bedrock surfaces in the Arroyo Chavez basin have higher average nuclide concentrations ($1.89 \pm 0.37 \times 10^5$ atoms g^{-1}) than other reservoirs. Fan deposits have lower average nuclide concentrations ($0.87 \pm 0.07 \times 10^5$ atoms g^{-1}), uncharacteristic of material that has been exposed for long periods of time and then stripped from the landscape prior to deposition.

Depth profile isotopic homogeneity. Nuclide concentrations in depth profiles of the alluvial deposits will record substantial changes in nuclide concentrations if erosion rates change over time. The basin alluvium profile (Fig. 6A) displays a regular increase in nuclide concentration with depth, consistent with postdepositional nuclide accumulation rather than substantial, erratic changes in concentration indicative of changes in basin-wide erosion rates over time.

Steady-state deposition. A basin, the uplands of which are eroding at a constant rate will accumulate sediment at a constant rate in if the rate of sediment generation is faster than the rate of sediment export. Isotopic data collected from the basin alluvium profile are consistent with steady-state deposition. We use the constant-deposition model of Lal and Arnold (1985) to approximate isotopic concentrations in sediments deposited in the basin over time:

$$N = C_i + \frac{P_0 \Lambda}{s\rho}\left(1 - e^{-(h\rho/\Lambda)}\right) \qquad (1)$$

In this relationship, nuclide concentration (N atoms g^{-1}) at a given depth (h cm) is a function of the initial nuclide concentration (C_i atoms g^{-1}), the production rate at the surface (P_0 atoms g^{-1} yr^{-1}), the characteristic attenuation coefficient for fast neutrons (Λ g cm^{-2}), the density of the overlying material (ρ g cm^{-3}), and the rate of sediment accumulation (s cm yr^{-1}).

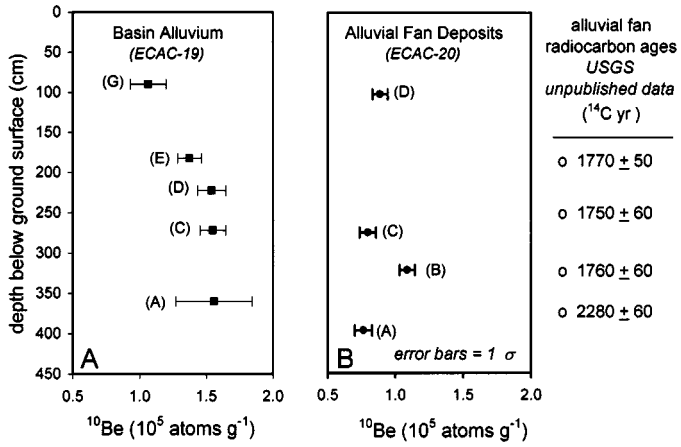

FIG. 6. ^{10}Be concentrations measured in basin alluvium and alluvial fan profiles. Radiocarbon dates from alluvial fan (○) are displayed along the right edge of the figure (USGS, M. Pavich, unpublished data). (A) Basin alluvium concentrations increase exponentially with depth, suggesting steady-state deposition. (B) Alluvial-fan nuclide concentrations do not change with depth, indicating a local, brief period of deposition.

Following deposition, grains of sediment continue to accumulate nuclides until they are buried deeply enough (200 to 300 cm) to be shielded from cosmic rays. Steady-state deposition produces a nuclide depth profile which is constant at depths greater than ~200 cm; nuclide abundance decreases with decreasing depth of burial (Fig. 7A). The basin alluvium depth profile we measured (Fig. 6A) is consistent with steady-state deposition and therefore with steady rates of sediment generation.

Assuming the nuclide abundance at the time of deposition was greater than or equal to the lowest concentration measured throughout the basin (~0.66×10^5 atoms g^{-1}, ECAC 14-1), we produced a series of curves representing model depth profiles at different sediment accumulation rates (Fig. 8). By visually fitting the measured data to the curves, we find the data correlate best with the curve representing a minimum limiting deposition rate of 280 m myr^{-1} ($\rho = 1.6$ g cm^{-3}), equivalent to 165 m myr^{-1} of upland bedrock erosion ($\rho = 2.7$ g cm^{-3}). This bedrock equivalent erosion rate is within one standard deviation of other estimates (Dethier *et al.*, 1988; Gellis *et al.*, 2000) and the calculations we describe later in this discussion (Table 3). The deposition rate we estimate indicates that sediment accumulation in the basin began ~13,000 yr B.P., consistent with late Pleistocene/early Holocene changes in climate and associated hydrologic controls on sediment generation and transport (Bull, 1991).

Although our model suggests steady-state erosion over the depositional history of the basin, our solution is not a unique explanation of the data. A systematic increase in rates of sediment deposition related to increased basinwide erosion rates could

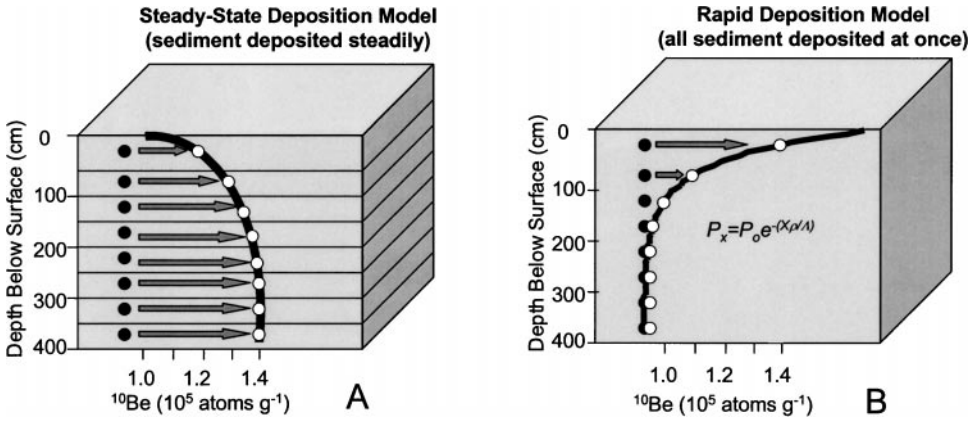

FIG. 7. Steady-state and rapid-deposition models for basin alluvium. (A) Sediment, deposited at a steady rate has an initial concentration determined by the erosion rate of upland source areas. If the basin is eroding steadily, all deposited sediment will have the same initial isotope concentration shown by the dark circles. As the sediment sits in storage and is slowly buried, it will accumulate atoms (arrows pointing to right) at a rate which decreases exponentially with burial depth. When sediment is buried 2 to 3 m, production approaches zero and accumulation stops (open circles). Particles higher in the profile will accumulate isotopes for a shorter period of time (deposited later) and thus will not yet have reached steady-state. (B) Sediment deposited rapidly will have initial concentrations that are homogenous with depth (black circles). Nuclides then accumulate based on the depth-production relationship (Lal, 1991), resulting in an exponentially decreasing depth profile (open circles).

account for the lower nuclide concentrations near the profile top. Alternatively, a recent stripping event depositing up to 100 cm of sediment in the basin could result in greater nuclide concentrations low in the profile (postdepositional nuclide accumulation) while recently deposited sediments near the top of the profile would have lower nuclide concentrations similar to the hillslope colluvium. However, stripping of the uplands would leave behind low-concentration (previously shielded) sediment and bedrock. The upland bedrock surfaces have the highest nuclide concentrations in the basin, suggesting long-term upland stability.

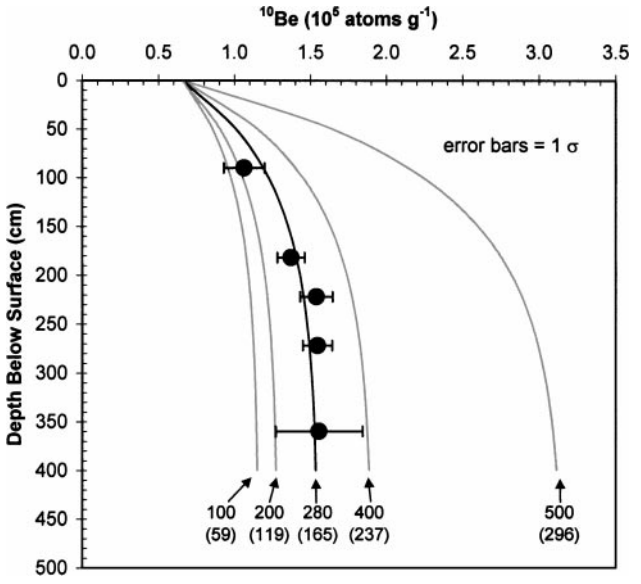

FIG. 8. Calculated isotopic depth profiles based on Eq. (1), the steady-state deposition model of Lal and Arnold (1985). Each curve represents a rate of deposition (m myr^{-1}) indicated beneath the curve. Numbers in parentheses are the associated bedrock-equivalent erosion rates (m myr^{-1}). Deposition rates are converted to erosion rates based on bedrock density of 2.7 g cm^{-3} and sediment density of 1.6 g cm^{-3}. An initial ^{10}Be concentration of 0.66×10^5 atoms g^{-1} was the lowest nuclide measurement in the basin, ECAC 14-1. Error bars represent 1σ analytical error.

On a smaller scale, the isotopic profile data collected from the alluvial fan show little variation with depth (Fig. 6B) suggesting rapid, recent deposition. Several radiocarbon dates taken in the alluvial fan profile (M. Pavich, USGS, previously unpublished data) demonstrate that the uppermost 300 cm were deposited in the last 1760 ± 60 ^{14}C yr B.P. (Fig. 6B). Although the average ^{10}Be concentration of the fan sediment is lower than the average of the hillslope colluvium, hillslope samples collected directly above the fan (ECAC14-1, -2, and -3), in an area of active incision, have average nuclide concentrations ($0.74 \pm 0.05 \times 10^5$ atoms g^{-1}) indistinguishable from the average fan nuclide concentrations ($0.87 \pm 0.07 \times 10^5$ atoms g^{-1}). These data illustrate the localized variations in erosion rates at the 1000 m^2 scale that are integrated by arroyo cycling. Although our data do not unequivocally prove steady-state erosion or a steady-state nuclide inventory, the three lines of evidence presented above indicate that the steady-state assumption is reasonable over the ~13,000-yr depositional history of the basin alluvium.

Lack of Grain Size Dependence

Arroyo Chavez data indicate that nuclide concentrations are independent of sediment grain size (Fig. 9). These data are consistent with measurements from other locations (Granger *et al.*, 1996; Clapp *et al.*, 2000); however, Brown *et al.* (1995a) found that the ^{10}Be concentration in river sediment from the Luquillo Experimental Forest, Puerto Rico, was inversely proportional to grain size due to different erosional mechanisms responsible for generating and transporting material of different sizes. Together, these studies suggest that the geomorphic processes

TABLE 3
Sediment-Generation Rates and Bedrock-Equivalent Lowering Rates for Arroyo Chavez Area, New Mexico

	^{10}Be & ^{26}Al in channel sediment	^{10}Be & ^{26}Al in hillslope colluvium	^{10}Be & ^{26}Al deposition model	Sediment budget[b]	Hypsometric calculation[c]
Sediment generation rate (g m^{-2} yr^{-1})	275 ± 65	402 ± 138	446 ± 140	394 ± 68	~270 ± na
Bedrock-equivalent lowering rate (m My^{-1})	102 ± 24	149 ± 51	165 ± 52	146 ± 25	~100 ± na
Effective time scale[a] (yr)	~10 to 20 ×10^3	~10 to 20 ×10^3	~10 to 20 ×10^3	2	1.1 ×10^6

[a] Amount of time over which calculations are integrated.
[b] Gellis *et al.* (2000).
[c] Dethier *et al.* (1988).

such as mass wasting or deep-seated land slides likely result in nuclide dependence on grain size. In a semiarid drainage, where sediments of many different sizes move by the slow processes of soil creep and surface wash, differential transport is less likely to occur and thus nuclide abundances are largely independent of grain size.

Erosion Rates, Sediment Generation, and Arroyo Cycling

Using cosmogenic ^{10}Be and ^{26}Al data, we have calculated basinwide, time-integrated rates of sediment generation for the Arroyo Chavez basin (Table 3). We present erosion rates as bedrock-equivalent lowering rates for comparison with other studies. The basinwide average erosion rate of 102 ± 24 m myr^{-1} (determined from arroyo channel sediments) is less than the rate determined by Gellis *et al.* (2000) from sediment traps on the Arroyo Chavez basin hillslopes (146 ± 25 m myr^{-1}) but similar to that determined by Dethier *et al.* (1988), who calculated retreat rates on hypsometric profiles of weakly lithofied sandstones in the nearby Western Espanola Basin (~100 m myr^{-1}). The difference between the nuclide-based erosion rate and the sediment-budget erosion rate (Gellis *et al.*, 2000) probably illustrates the importance of integration time (10^1 vs 10^3 yr) and scale (10^3 m^2 vs 10^6 m^2). Interestingly, the nuclide-based erosion rate determined only from hillslope colluvium samples (149 ± 51 m myr^{-1}) is very similar to that of Gellis and Aby (146 ± 25 m myr^{-1}).

The erosion rate we have determined for Arroyo Chavez (102 ± 24 m myr^{-1}) is substantially greater than bedrock rates measured in more arid regions with more erosion-resistant bedrock and less soil development, such as south-central Australia, ~0.6 to 6 m myr^{-1} (Bierman and Turner, 1995), and Antarctica, ~0.1 to 1.0 m myr^{-1} (Nishiizumi *et al.*, 1991). Our higher erosion rates are consistent with an easily eroded lithology in a slightly wetter climate (semiarid) and in a location where mechanical weathering is more prevalent. Our estimates are also consistent with more general, large-scale rates determined for the Colorado Plateau of 165 and 83 m myr^{-1} by Judson and Ritter (1964) and Holeman (1968), respectively.

Both our cosmogenic data and the physical data collected by Gellis *et al.* (2000) indicate that hillslopes are eroding faster than more resistant bedrock uplands. The average nuclide activity in bedrock outcrops (1.89 ± 0.37 ×10^5 atoms g^{-1}) is greater (90% confidence) than that of hillslope samples (1.10 ± 0.18 × 10^5 atoms g^{-1}), as would be expected when comparing the most resistant materials in the basin (mesa-forming sandstones) to less resistant materials (slope-forming interbedded sandstones and shales). Based on the isotopic evidence for higher hillslope erosion rates and the greater basin slope area than outcrop area (<5% of the basin contributing area is exposed bedrock), our measurements indicate that bedrock-to-soil conversion on the hillslopes generates substantially more sediment within the basin than does erosion of bedrock outcrops. Our findings of greater rates of regolith production beneath a cover of colluvium are consistent with previous works (Gilbert, 1877; Bull, 1991; Small *et al.*, 1999) suggesting that, in more arid environments, colluvium retains moisture from infrequent precipitation events that, when held in contact with bedrock, facilitates chemical and mechanical weathering. In more humid regions, such as those described by Heimsath *et al.* (1997, 1999), colluvium appears to hinder the production of regolith.

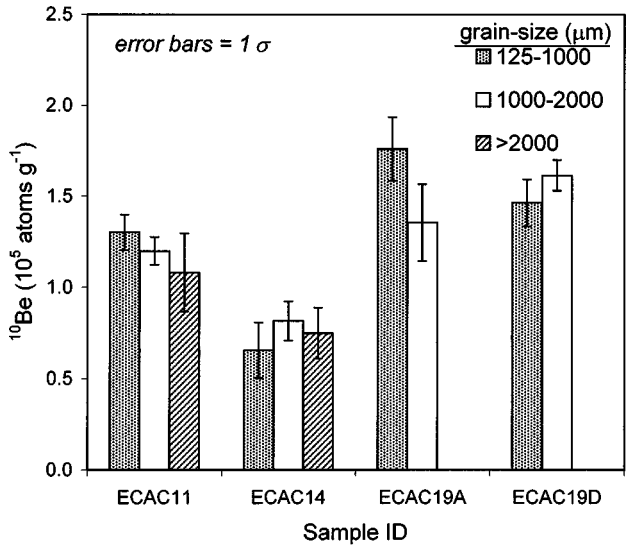

FIG. 9. ^{10}Be concentrations for different sediment grain size fractions of four samples. Nuclide concentration is independent of grain size.

We have calculated a basinwide, average sediment generation rate (275 ± 65 g m^{-2} yr^{-1}) based on nuclide concentrations in channel sediment. Using the present-day sediment-contributing area of the basin (0.51 km^2) and an estimated maximum sediment volume of the present-day arroyo cut ($\sim$20,000 m^3, length of the arroyo and tributaries multiplied by average width and depth of the channel), the total volume of sediment generated (88 m^3 yr^{-1} based on a sediment density of 1.6 g cm^{-3}) is sufficient to fill the present-day arroyo approximately once every 230 years. This calculation assumes that no sediment is exported from the basin during filling (e.g., a 100% trapping efficiency) and that the net aeolian contribution is negligible (estimated at $<$1% by Gellis *et al.* (2000)). However, estimates of even 50 to 75% sediment export would allow arroyo backfilling roughly every 1000 years. Our data therefore show that in this small, high-elevation, semiarid basin, sufficient sediment is generated from the hillslopes to fill the current arroyo and perpetuate the arroyo cycles that have recurred several times during the past 3000 years (Elliott *et al.*, 1999).

CONCLUSIONS

Measurements of ^{10}Be and ^{26}Al in the sediment and bedrock of the Arroyo Chavez basin indicate that the basin is in long-term erosional steady-state, that fluvial sediment is isotopically representative of the basin as a whole, that grain size does not control nuclide abundance, and that sufficient sediment is produced (275 ± 65 g m^{-2} yr^{-1}) to support rapid arroyo cycling. The long-term bedrock-equivalent basin-scale lowering rate (102 ± 24 m myr^{-1}) we calculate is in good agreement with other regional denudation estimates and local short-term measurements of sediment generation. Differences in nuclide concentrations measured in bedrock and hillslope colluvium indicate that weathering of subcolluvial bedrock generates more sediment than weathering of exposed bedrock.

ACKNOWLEDGMENTS

U.S. Geological Survey Grant HQ96AG01589, NSF Grant EAR-9628559, and Department of Energy Contract W-7405-ENG-48 supported this work. We thank M. Abbott, A. Gellis, and S. Aby for field assistance, S. Nies and K. Marsella for lab assistance, E. A. Cassell, R. Stanley, D. Wang, S. Gran, A. Noren, K. Jennings, and D. Santos for reviews, and J. Sevee and P. Maher for support.

REFERENCES

Aby, S. B. (1997). Date of channel trenching (arroyo cutting) in the arid Southwest revisited. *Geological Society of America Abstracts with Programs* **29,** 373.

Bierman, P., and Steig, E. (1996). Estimating rates of denudation and sediment transport using cosmogenic isotope abundances in sediment. *Earth Surface Processes and Landforms* **21,** 125–139.

Bierman, P. R., and Turner, J. (1995). ^{10}Be and ^{26}Al evidence for exceptionally low rates of Australian bedrock erosion and the likely existence of pre-Pleistocene landscapes. *Quaternary Research* **44,** 378–382.

Brown, T. B., Stallard, R. F., Larsen, M. C., Raisbeck, G. M., and Francoise, Y. (1995a). Denudation rates determined from accumulation of in situ-produced ^{10}Be in the Luquillo Experimental Forest, Puerto Rico. *Earth and Planetary Science Letters* **129,** 193–202.

Brown, E. J., Bourles, D. L., Colin, F., Raisbeck, G. M., Yiou, F., and Desgarceaux, S. (1995b). Evidence for muon-induced production of ^{10}Be in near surface rocks from the Congo. *Geophysical Research Letters* **22,** 703–706.

Bryan, K. (1925). Date of channel trenching in the arid Southwest. *Science* **62,** 338–344.

Bull, W. B. (1991). "Geomorphic Responses to Climate Change." Oxford Univ. Press, New York.

Clapp, E. M., Bierman, P. R., Schick, A. P., Lekach, J., Enzel, Y., and Caffee, M. (2000). Sediment yield exceeds sediment production in arid region drainage basins. *Geology* **28,** 995–998.

Clark, D. H., Bierman, P. R., and Larsen, P. (1995). Improving in situ cosmogenic chronometers. *Quaternary Research* **44,** 366–376.

Cooke, R. U., and Reeves, R. W. (1976). "Arroyos and Environmental Change in the American Southwest." Clarendon, Oxford.

Dethier, D. P., Harrington, C. D., and Aldrich, M. J. (1988). Late Cenozoic rates of erosion in the western Espanola basin, New Mexico—Evidence from geologic dating of erosion surfaces. *Geological Society of America Bulletin* **100,** 928–937.

Elliott, J. G., Gellis, A. C., and Aby, S. B. (1999). Evolution of arroyos: Incised channels of the southwestern United States. *In* "Incised River Channels" (S. E. Dorby and A. Simon, Eds.), pp. 153–185. Wiley, Chichester.

Gellis, A. C., Pavich, M. J., Bierman, P. R., Ellwein, A., Aby, S., and Clapp, E. M. (2000). Measuring erosion rates using modern geomorphic and isotopic measurements in the Rio Puerco, New Mexico. *Geological Society of America Abstracts with Programs* **32,** 207.

Gellis, A. C., and Elliott, J. G. (1998). Arroyo changes in selected watersheds of New Mexico, United States. *In* "Applying Geomorphology to Environmental Management, a Special Publication Honoring Stanley A. Schumm" (M. Harvey and D. Anthony, Eds.), pp. 271–284. Water Resources Publications, LLC, Highlands Ranch, CO.

Gilbert, G. K. (1877). Geology of the Henry Mountains (Utah): U.S. Geographical and Geological Survey of the Rocky Mountains Region, 160 pp.

Granger, D. E., Kirchner, J. W., and Finkel, R. (1996). Spatially averaged long-term erosion rates measured from in-situ produced cosmogenic nuclides in alluvial sediment. *Journal of Geology* **104,** 249–257.

Heimsath, A. M., Dietrich, W. E., Nishiizumi, K., and Finkel, R. C. (1999). Cosmogenic nuclides, topography, and the spatial variation of soil depth. *Geomorphology* **27,** 151–172.

Heimsath, A. M., Dietrich, W. E., Nishiizumi, K., and Finkel, R. C. (1997). The soil production function and landscape equilibrium. *Nature* **388,** 358–361.

Holeman, J. N. (1968). The sediment yield of major rivers of the world. *Water Resources Research* **4,** 737–747.

Judson, S., and Ritter, D. F. (1964). Rates of regional denudation in the United States. *Journal of Geophysical Research* **69,** 3395–3401.

Kohl, C. P., and Nishiizumi, K. (1992). Chemical isolation of quartz for measurement of in-situ-produced cosmogenic nuclides. *Geochimica et Cosmochimica Acta* **56,** 3583–3587.

Lal, D. (1988). In situ-produced cosmogenic isotopes in terrestrial rocks. *Annual Reviews of Earth and Planetary Science* **16,** 355–388.

Lal, D. (1991). Cosmic ray labeling of erosion surfaces: *In situ* production rates and erosion models. *Earth and Planetary Science Letters* **104,** 424–439.

Lal, D., and Arnold, J. R. (1985). Tracing quartz through the environment. *Proceedings of the Indian Academy of Science (Earth and Planetary Science)* **94,** 1–5.

Leopold, L. B., Emmett, W. W., and Myrick, R. M. (1966). "Channel and Hillslope Processes in a Semiarid Area, New Mexico." U.S. Geological Survey Professional Paper 352-G, pp. 193–253.

Love, D. W. (1986). A geological perspective of sediment storage and delivery along the Rio Puerco. *In* "Drainage Basin Sediment Delivery" (R. F. Hadley, Ed.), IAHS Publication 159, pp. 305–322. Wallingford, UK.

Love, D. W., and Young, J. D. (1983). Progress report on the late Cenozoic geologic evolution of the lower Rio Puerco. *In* "New Mexico Geological Society Guidebook 34, Socorro Region II". (C. E. Chaplin, Ed.). pp. 277–284, New Mexico Geological Society (publisher), Socorro, NM.

Nishiizumi, K., Kohl, C. P., Arnold, J. R., Klein, J., Fink, D., and Middleton, R. (1991). Cosmic ray produced ^{10}Be and ^{26}Al in Antarctic rocks: Exposure and erosion history. *Earth and Planetary Science Letters* **104,** 440–454.

Nishiizumi, K., Winterer, E. L., Kohl, C. P., Klein, J., Middleton, R., Lal, D., and Arnold, J. R. (1989). Cosmic ray production rates of ^{10}Be and ^{26}Al in quartz from glacially polished rocks. *Journal of Geophysical Research* **94,** 17907–17915.

Ott, R. L. (1993). "An Introduction to Statistical Methods and Data Analysis." Wadsworth, Belmont, CA.

Reheis, M. C., and Kihl, R. (1995). Dust deposition in southern Nevada and California, 1984–1989: relations to climate, source area and source lithology. *Journal of Geophysical Research* **100,** 8893–8918.

Sharma, P., and Middleton, R. (1989). Radiogenic production of ^{10}Be and ^{26}Al in uranium and thorium ores: Implications for studying terrestrial samples containing low levels of ^{10}Be and ^{26}Al. *Geochimica et Cosmochimica Acta* **53,** 709–716.

Small, E. E., Anderson, R. S., and Hancock, G. S. (1999). Estimates of the rate of regolith production using ^{10}Be and ^{26}Al from an alpine slope. *Geomorphology* **27,** 131–150.

U.S. Geological Survey (1961). "San Luis, New Mexico Quadrangle." USGS, Reston, VA.

York, D. (1969). Least-squares fitting of a straight line with correlated errors. *Earth and Planetary Science Letters* **5,** 320–324.